33RD CONGRESS
OF THE INTERNATIONAL COUNCIL
OF THE AERONAUTICAL SCIENCES
STOCKHOLM, SWEDEN, 4-9 SEPTEMBER, 2022

ICAS 2022 SWEDEN

EXPERIMENTAL STUDIES ON THE INTERACTION BETWEEN PROPELLERS AND WING

Gabriel Pereira Gouveia da Silva[1], Marcos Vítor de Rosa Jacinto da Silva[1], João Paulo Eguea[1] & Fernando Martini Catalano[1]

[1]Department of Aeronautical Engineering, University of Sao Paulo, Brazil

Abstract

The aerodynamic and aeroacoustic interaction effects between propellers and between propellers and wing are being investigated experimentally in a wind tunnel at the Department of Aeronautical Engineering of the University of São Paulo (Brazil). The results will bring a better understanding of these interactions, which will allow the elaboration of good practices for distributed electric propulsion conceptual designs, and provide a database for validating computational tools. The experimental setup, methods, and some preliminary acoustic results are shown in this paper.

Keywords: Distributed electric propulsion. DEP. Aerodynamics. Aeroacoustics. Wind tunnel testing.

1. Introduction

Inherent characteristics of electric motors, such as high efficiency, reduced volume, low weight, power independence to altitude, and the ability to scale over a wide range of sizes without loss of efficiency or weight-power ratio make electric motors suitable for aeronautical propulsion [1, 2, 3, 4]. In addition, electric motors allow new degrees of freedom for aeronautical designers to position the engines to obtain better aeropropulsive integration, in such a way that the efficiency of the set is greater than the sum of the individual efficiencies [1, 2, 3, 4].

Traditionally, however, propellers and wings are designed independently, since the interactions between them are quite complex [5, 6, 7]. During the conceptual design phase of both, the aerodynamic interactions between propellers and wing and between propellers are not well modeled (only empirical corrections of installation effects can be made) [7]. More details about these interactions, in this traditional design philosophy, are obtained through more expensive tools such as CFD (Computational Fluid Dynamics), CAA (Computational AeroAcoustics), and wind tunnel testing campaigns, when most of the concept is already frozen and the designer does not have much creative freedom to change it [5, 1, 7].

Although this approach is sufficiently suitable for the design of conventional propeller-driven aircraft, the same is not true for the design of new aircraft that make use of DEP (Distributed Electric Propulsion), in which the synergistic effects of aeropropulsive integration are an essential part of the concept [7]. This is because the existing empirical and semi-empirical methods are limited to experimental datasets of already manufactured traditional aircraft, which in general do not account for this synergistic influence between wings and propellers [1, 7]. Wang et al. [8] also point out that there is a lack of publications in the literature that show how to apply existing knowledge about the interaction phenomena present in the flow of a wing with an installed propeller to the aerodynamic design of wings and propellers, which indicates the need to research this topic to meet the growing demand in the sector. According to Kroo [9], efficient integration between propeller and wing is a problem as important as it is difficult, which also reinforces the need for research on the subject. In this context, an emerging topic of research is the development of numerical methods that can capture the effects of these interactions at a low computational cost to be used during the initial phases of the

project, allowing a better exploration of the design space in optimization loops, for example. The models developed by Alvarez and Ning [10, 11, 12] and by Cole [1] and Cole et al. [7] are some examples of these new computational techniques applied to the simulation of the interaction effects between propellers and wings. However, for these new methods to be useful for DEP aircraft design and optimization, they must be able to correctly predict the experimentally verified phenomena and trends. To allow this validation and promote a better understanding of the interaction phenomena, a DEP test rig was built at the Department of Aeronautical Engineering of the University of São Paulo (Brazil) and a test campaign is being carried out to compile a database of experimental data that correlate parameters such as the relative position of the propellers to the wing with the propulsive and aerodynamic performance. Some of the preliminary tests and results are shown in this paper.

2. Methods

The wind tunnel in which the acoustic measurements are being carried out is an open circuit blower with an open test section located at the facilities of the Department of Aeronautical Engineering of the University of Sao Paulo. This tunnel has a rectangular section jet measuring $1.04\ m$ (width) × $0.79\ m$ (height), with a freestream airspeed of up to $24\ m/s$ and turbulence level to be measured.

To carry out this research project, a chamber coated with polyurethane foam wedges was built around the wind tunnel jet (Fig. 1) to allow the execution of acoustic measurements in an acoustic field closer to the ideal (free and with low reverberation time).

The chamber's acoustic performance was evaluated by using 5 microphone paths and an omnidirectional sound source emitting pink noise (Fig. 1). In the tests to verify the decay of sound intensity with the square of the distance to the source, pink noise was emitted continuously, whereas in the tests of reverberation time, a pulse of pink noise was emitted. The reverberation time RT60 was measured from the extrapolation of the reverberation time RT20 (Fig. 2) and it was calculated for octave bands (Fig. 3). Considering that the internal volume of the chamber is $31.6\ m^3$, according to Long [13], the measured reverberation time values place the chamber in a range suitable for recording and broadcasting studios for speech. In case of the propellers tested in this research, their blade passing frequencies (BPF) are contained in the octave band centered at $250\ Hz$, whose RT60 is $0.217\ s$, being adequate so that the measurements of interest are not heavily contaminated by reverberation.

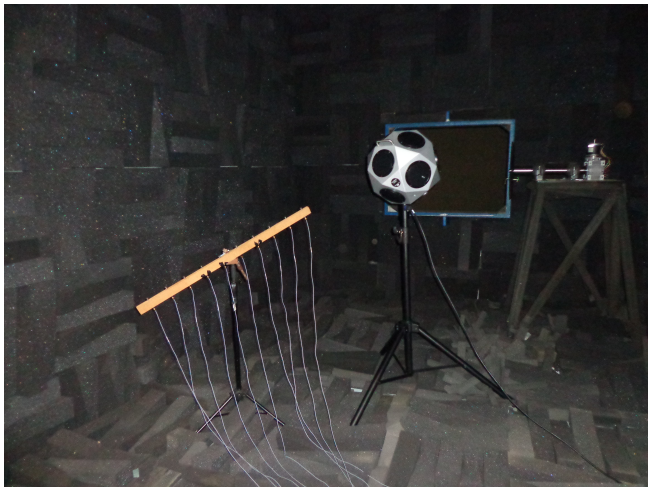

Figure 1 – Acoustically treated test chamber, with the omnidirectional sound source and one of the five microphone paths to test the chamber acoustic performance.

The wind tunnel in which lift, drag, pitch moment, surface pressure scanning, and wake mapping will be carried out is the LAE-1 tunnel, installed at the Laboratory of Experimental Aerodynamics (LAE) of the Department of Aeronautical Engineering of the University of Sao Paulo. This tunnel has a closed circuit and test section, which allows flow speeds of up to $50\ m/s$ with a turbulence level of 0.21% in its rectangular test section of $1.67\ m$ (width) × $1.29\ m$ (height) × $3\ m$ (length). Although this tunnel has a microphone array, its walls are acoustically rigid, making acoustic measurements that are not

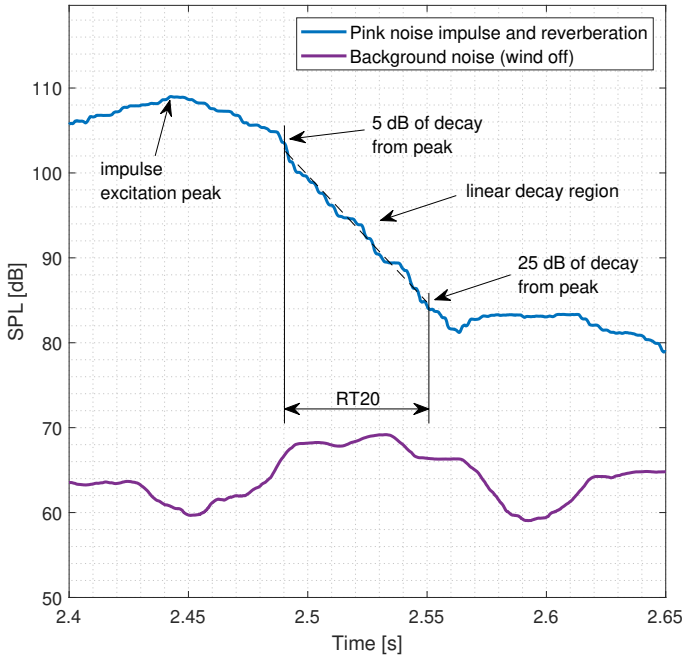

Figure 2 – Variation of sound intensity level with time after a pink noise pulse.

made through beamforming techniques (which increase the signal/noise ratio) unsuitable for noise measurements from rotating sources.

The test rig consists of a three-dimensional wing (Fig. 4) machined from aluminum alloy with fittings for up to 3 electric motors, whose positions are fixed in the spanwise direction and adjustable in the chordwise direction and in a direction perpendicular to the chord-span plane. The wing has a span of $700\ mm$ and a $400\ mm$ chord, with an airfoil section developed in previous research carried out at LAE [14]. The wing has 62 pressure taps distributed along the span at a position of 30% of the chord for surface pressure scanning, aerodynamic torque and thrust balances for propellers (designed by Silva, Eguea and Catalano [15], Fig. 5, 6 and 7) and hinge moment balance for the aileron, flap with two positions (retracted and $30°$) and aileron with 6 positions ($-15°$, $-10°$, $-5°$, $0°$, $+5°$ and $+10°$). The flap has a span of 70% of the wingspan and a chord of 25% of the wing chord, while the aileron has a span of 25% of the wingspan and a chord of 25% of the wing chord. The model has an interchangeable fixture that allows it to be installed on an open-section wind tunnel endplate or on the LAE-1 wind tunnel aerodynamic balance. A positioning support composed of a worm gear

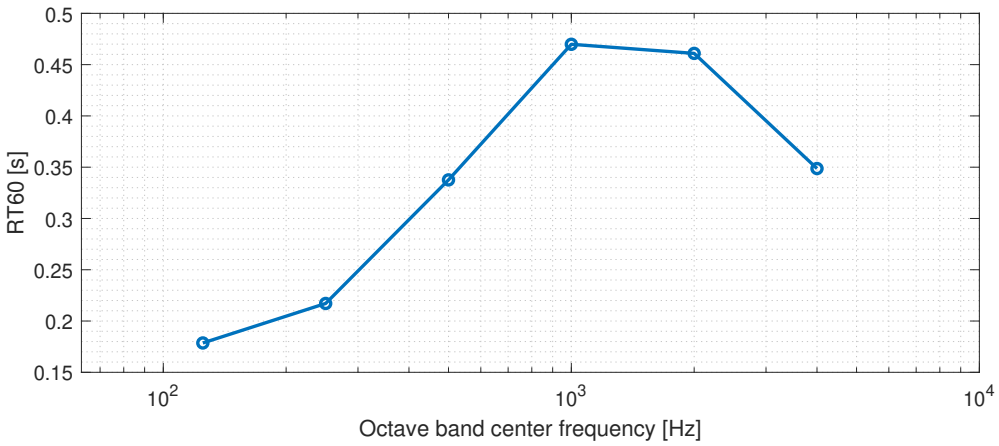

Figure 3 – Reverberation time inside the chamber for different octave bands.

reducer and a stepper motor is responsible for the angular positioning of the model in relation to the airflow of the open jet wind tunnel (Fig. 4).

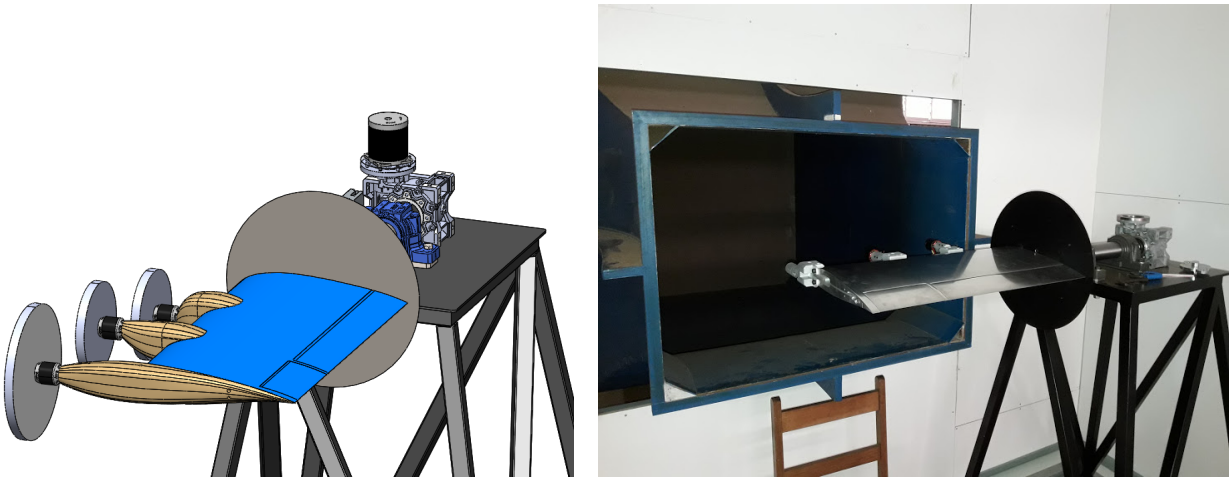

(a) (b)

Figure 4 – Model positioning support and wnig, from design to final construction.

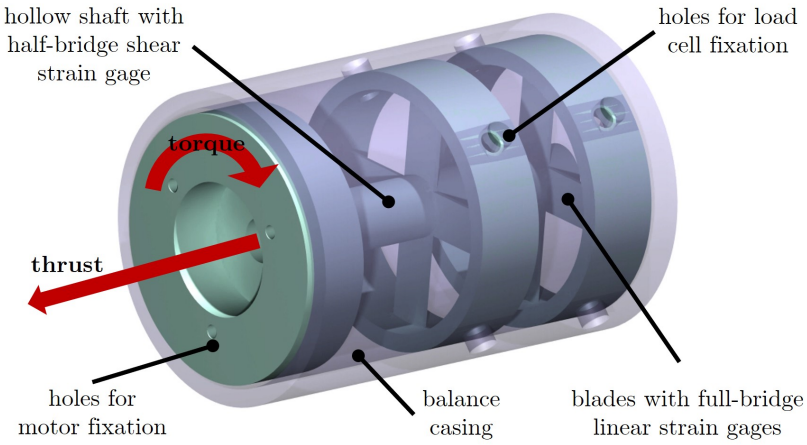

Figure 5 – Details of the balance designed by the authors to measure the thrust and torque of a propeller. Source: [15]

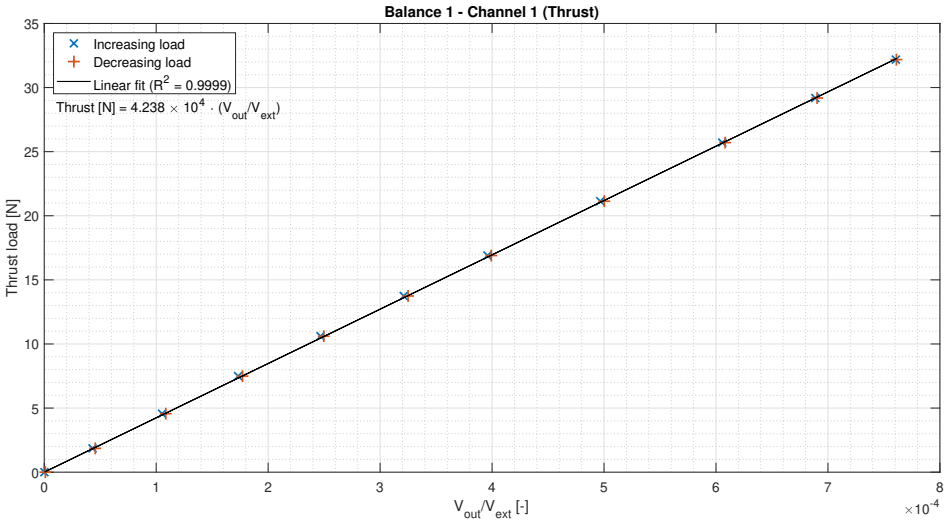

Figure 6 – Propeller thrust transducer calibration curve and hysteresis.

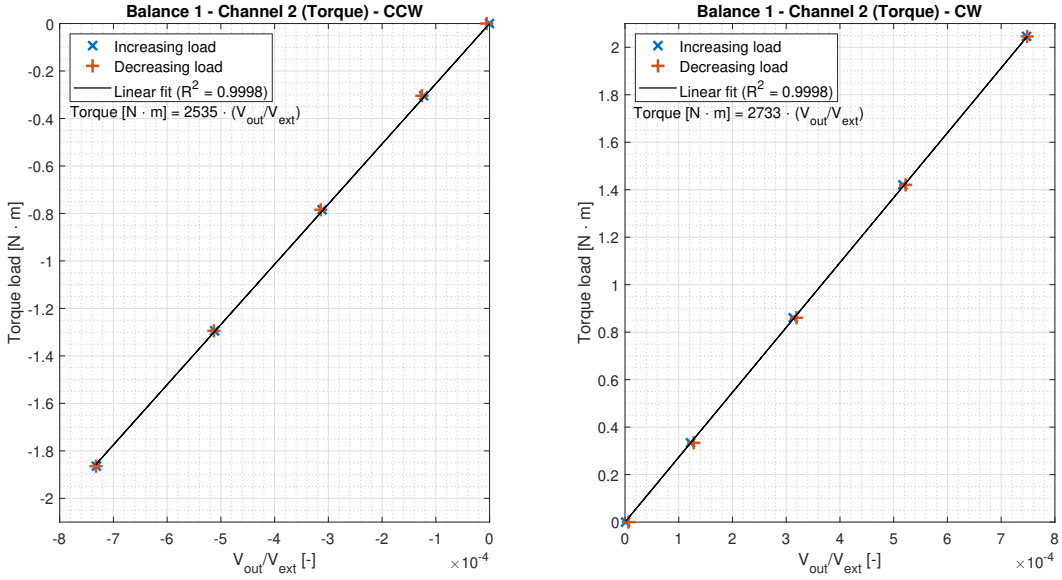

Figure 7 – Propeller torque transducer calibration curve and hysteresis

Considering the objective of compiling an extensive database that allows the correlation between parameters relevant to the aeropropulsive and aeroacoustic performance of propellers installed in DEP aircraft, the following parameters of interest were selected:

- **Controlled input parameters:** constructive and operational parameters of the propellers (airfoil, diameter, pitch, advance ratio, installation vertical position and installation position in the chordwise direction; flow data (angle of attack, Reynolds and Mach numbers); wing configuration (number of installed propellers, flap deflection and aileron deflection).
- **Uncontrolled but measured input parameters:** atmospheric data (temperature, relative humidity, atmospheric pressure, air density, and viscosity).
- **Output parameters measured:** Mach number at the tip of the propellers; time series of acoustic pressure in the microphone array; torque and thrust in each propeller-motor assembly; aileron hinge moment; wing lift, drag and pitch moment; wake pressure maps; total pressure on the model surface in a line in the spanwise direction.

	Tip propeller position					
	1,1	1,2	2,1	2,2	3,1	3,2
x_p/c	0.53	0.42	0.53	0.42	0.53	0.42
y_p/c	0.07	0.07	0.02	0.02	−0.03	−0.03

Table 1 – Wingtip propeller positions.

The combinations of controlled input parameters will be based on the typical characteristics of the flight phases of interest (takeoff, climb, and cruise) with regard to the values of advance ratios, angles of attack, and propeller configurations. The test matrix containing all these combinations is in elaboration and the expected results are plots relating these inputs and outputs.
For the preliminary tests presented in this article, two commercial propellers were compared (APC 14×6P and APC 12×6EP), installed counter-rotating to the wingtip vortex in 6 different positions in relation to the wing, as shown in Fig.8 and Tab. 1 The wing was tested at an angle of attack of $3°$, average Mach of 0.06 and average Reynolds of 4.67×10^5, with the APC 14×6P propeller operating at 4400 RPM and the APC 12×6EP propeller operating at 5500 RPM. The acoustic measurements and acquisition was performed at 51200 samples per second during 30 seconds using 10 Brüel & Kjaer Type 4944-B pressure-field microphones connected to a National Instruments PXIe-4497 acquisition board. The microphone array was arranged in a straight line in the direction of airflow, positioned at the central line of the wind tunnel on the floor of the acoustic chamber, in grazing incidence.
Although the results shown in the next section refer to the measurements of a single microphone, located just below the model, the measurements made with the 10 microphones will allow, for example, the calculation of the directivity of the noise sources, providing a better understanding of the aeroacoustic phenomena studied and a greater wealth of information for validating CAA simulations.

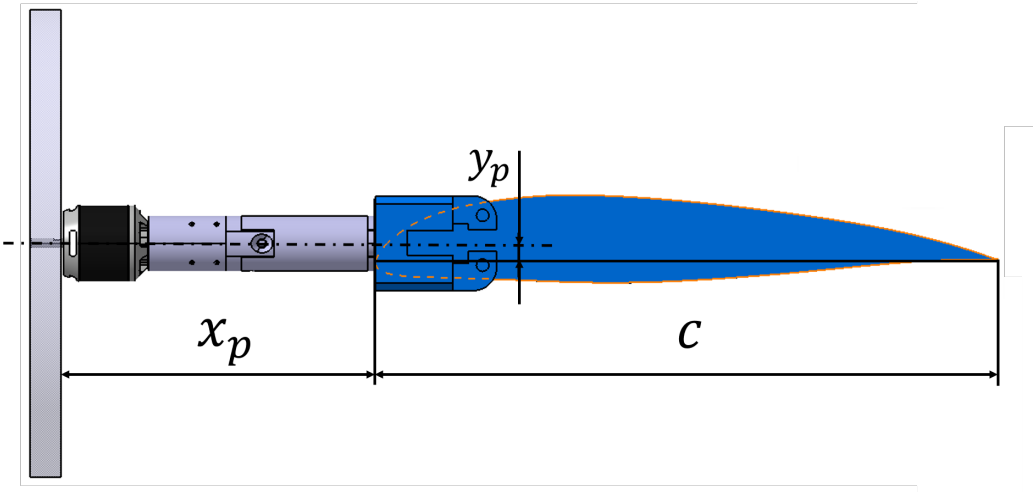

Figure 8 – Wingtip propeller positions.

3. Results

The results, measured as indicated in the previous section, were processed using the Welch method with Hanning windowing (blocks with 8192 samples and 75% of block overlapping, with power correction factor of 8/3). These settings allow a spectral analysis between the frequencies of $3.125\ Hz$ and $25600\ Hz$, with a resolution of $3.125\ Hz$. The narrowband acoustic spectra for each propeller in each position are shown in Figures 9,10,11,12,13,14,15, and 16.

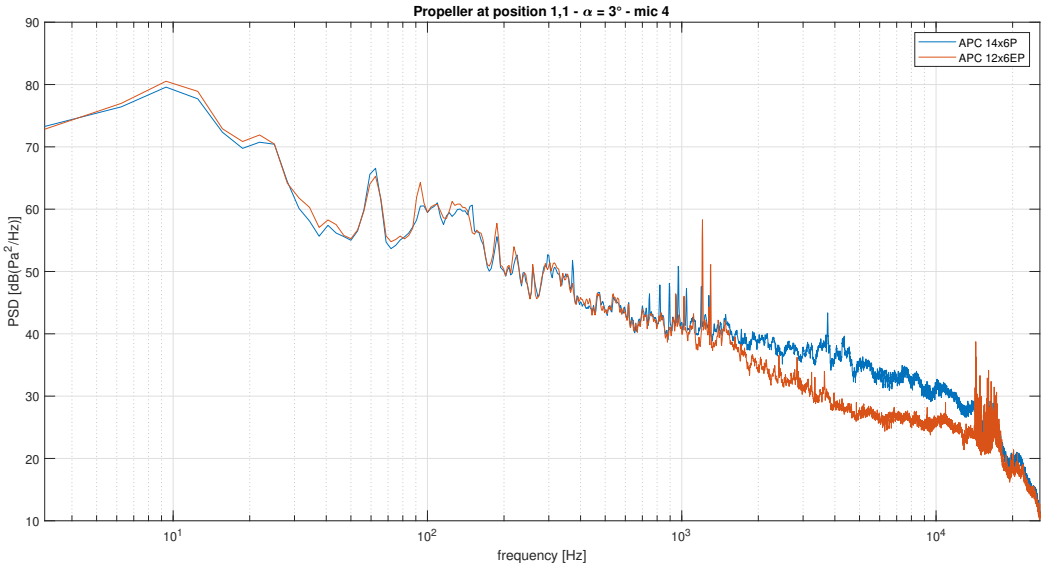

Figure 9 – Narrowband noise spectra for propellers installed at position 1,1.

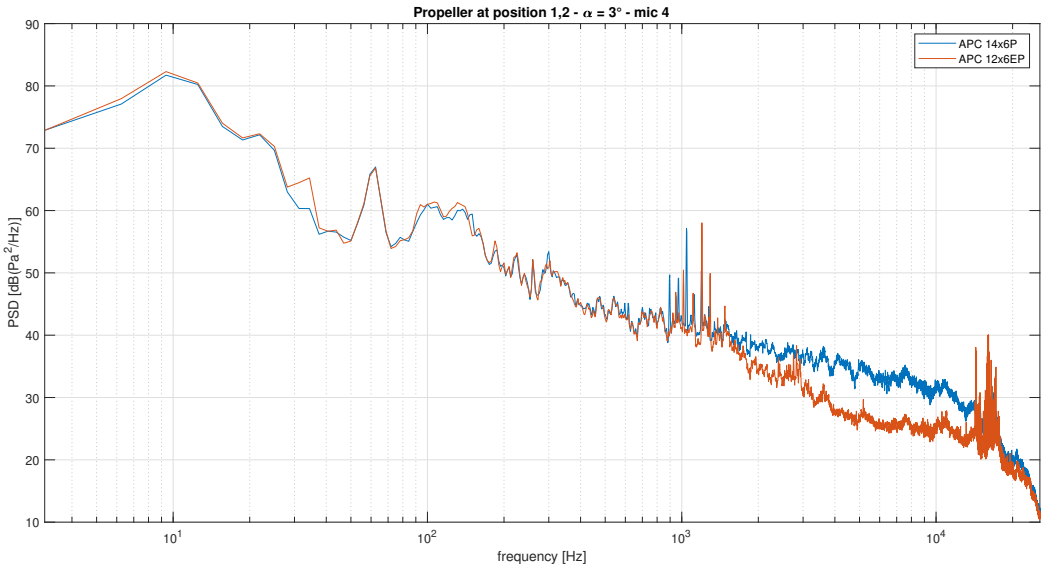

Figure 10 – Narrowband noise spectra for propellers installed at position 1,2.

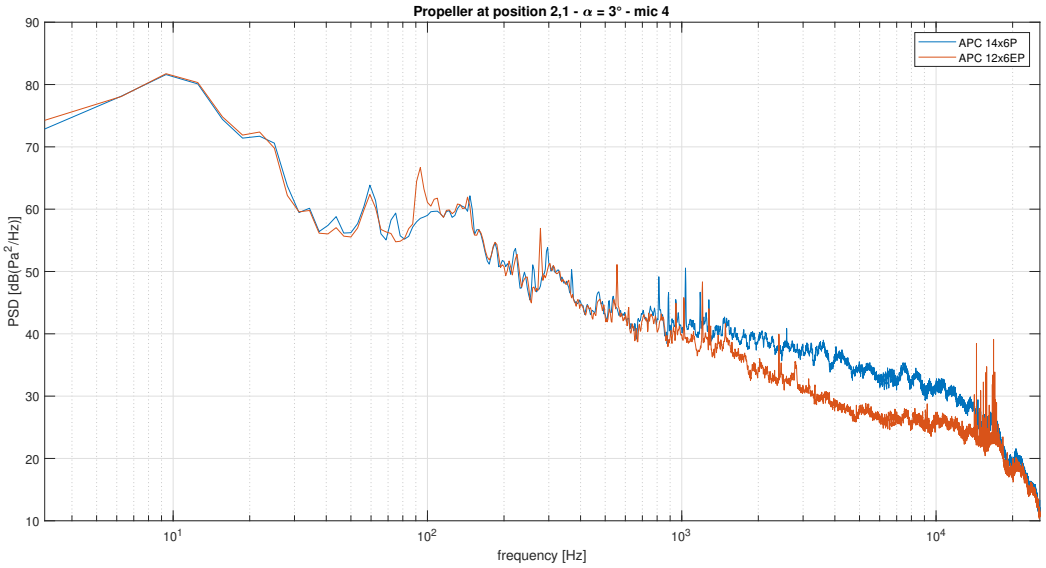

Figure 11 – Narrowband noise spectra for propellers installed at position 2,1.

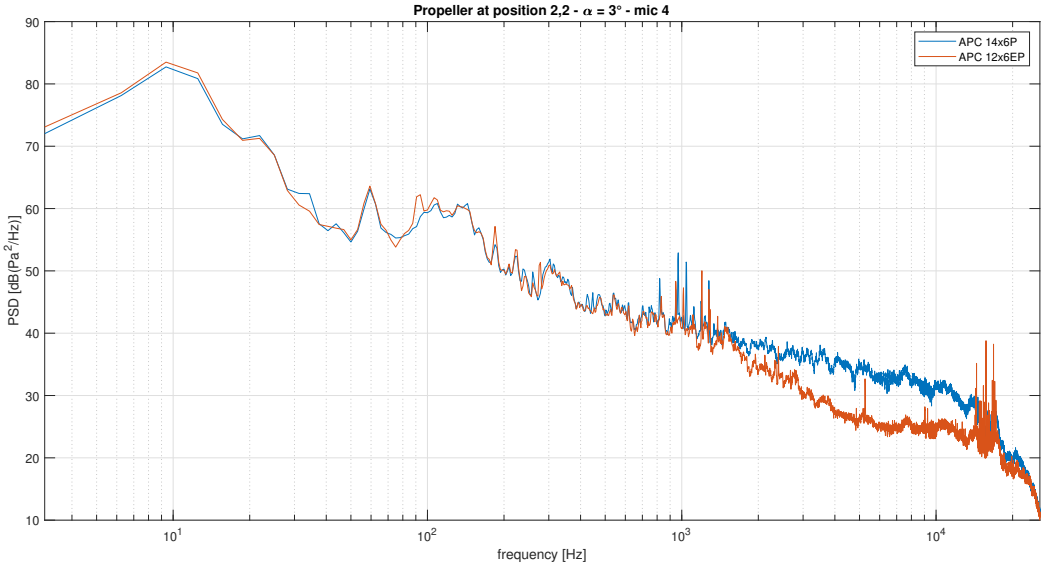

Figure 12 – Narrowband noise spectra for propellers installed at position 2,2.

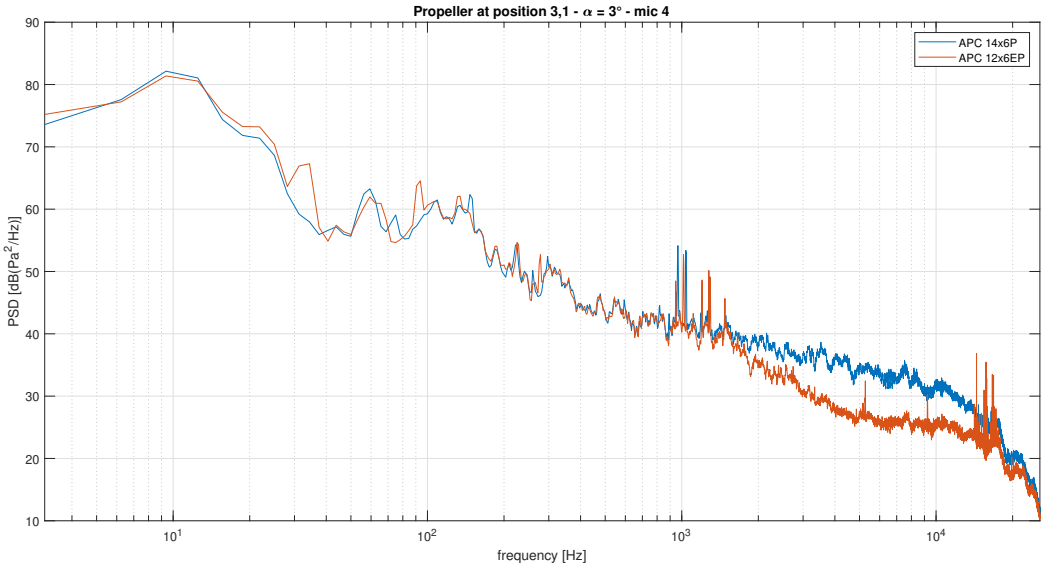

Figure 13 – Narrowband noise spectra for propellers installed at position 3,1.

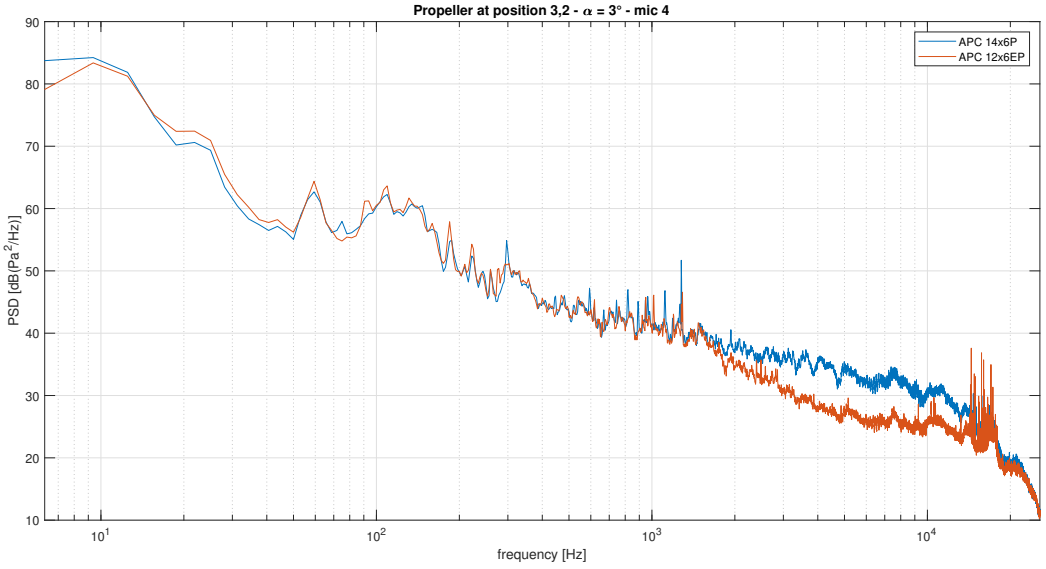

Figure 14 – Narrowband noise spectra for propellers installed at position 3,2.

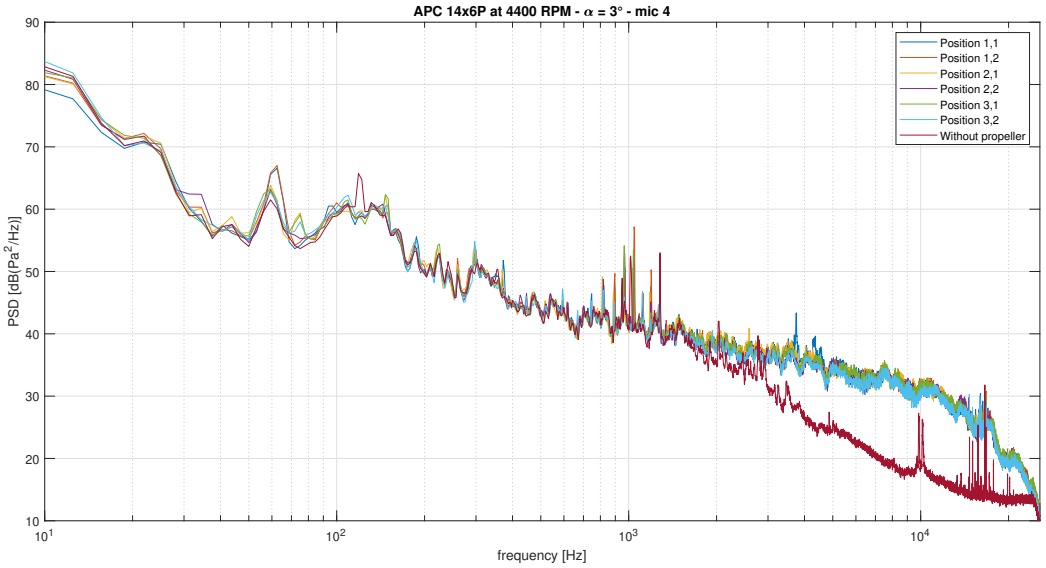

Figure 15 – Narrowband noise spectra for the APC 14×6P installed at different positions.

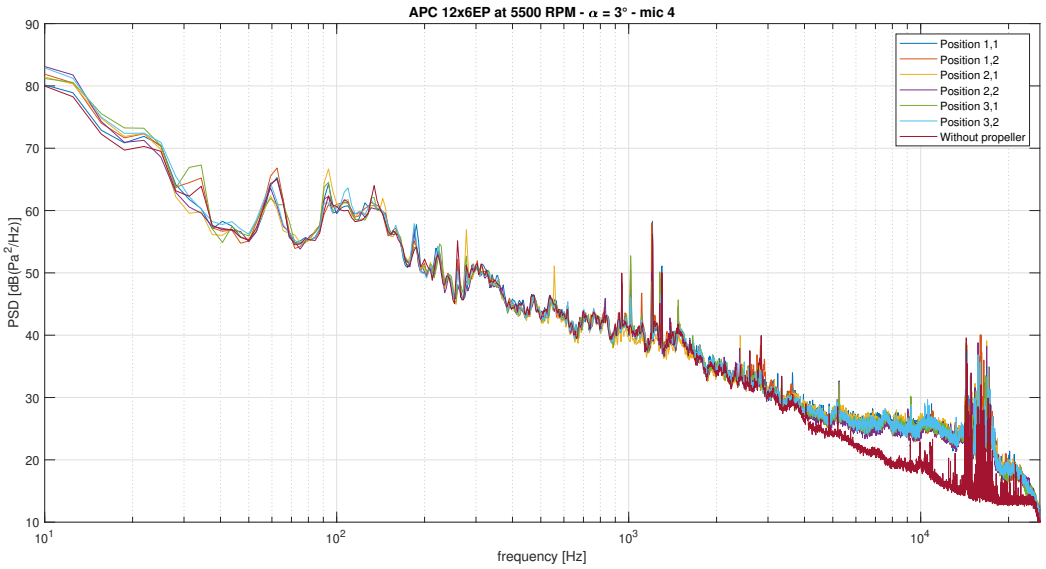

Figure 16 – Narrowband noise spectra for the APC 12×6EP installed at different positions.

4. Discussion and next steps

It is possible to notice from the preliminary results that above $2\ kHz$ the larger propeller produces more broadband noise than the smaller propeller. This component of the propeller noise is more difficult to model and control than the tonal noise of BPF, having a component that behaves like an acoustic dipole and that is related to the detachment of vortices with different periodicities in the trailing edge of the blades according to the speed and thickness at each radial blade position; and another component that behaves like an acoustic quadrupole and is related to the turbulence produced in the shear layer between the propeller jet and the air that is around it [16]. In addition, conditions such as non-uniformity, turbulence, or inclination of the inflow in relation to the propeller disk are also important sources of broadband noise [16].

For the analyzed microphone, the BPF and its harmonics do not stand out much in relation to broadband noise. For future analyzes in which can be interesting to evaluate the BPF tonal noise, it will be necessary to verify if the other microphones in the array can better capture this tonal noise components, or even use techniques for separating deterministic and non-deterministic noise sources, such as ensemble averaging techniques (which are possible to apply with the setup used in this research, since the propeller phase measurement through a photoelectric sensor is synchronized with the microphone measurements).

The next steps of this research include measurements of propeller thrust force and torque, as well as measurements of lift, drag, and pitch moment of the wing with the cruise propeller, as well as processing the acoustic measurements of all the microphones of the array to estimate directivity and other aeroacoustic parameters of interest.

5. Contact Author Email Address

mailto: gabriel.gouveia.silva@alumni.usp.br

6. Copyright Statement

7. Acknowledgments

The authors thank the National Council for Scientific and Technological Development (CNPq) [grant number 140352/2019-8] and to Embraer S.A. for the financial support given to this research; and the engineering team of Embraer S.A. for their technical and scientific support in the development of the experimental setup and techniques.

References

[1] Cole J. A. *A higher-order free-wake method for aerodynamic performance prediction of propeller-wing systems*. PhD Thesis, The Pennsylvania State University, 2016.

[2] Patterson M. D., Borer N. K. and German B. A simple method for high-lift propeller conceptual design. *54th AIAA Aerospace Sciences Meeting*, 2016.

[3] Kim H. D., Perry, A. T., Ansell, P. J. A review of distributed electric propulsion concepts for air vehicle technology. *2018 AIAA/IEEE Electric Aircraft Technologies Symposium*, 2018.

[4] Marcus E. A. et al. Aerodynamic investigation of an over-the-wing propeller for distributed propulsion. *2018 AIAA Aerospace Sciences Meeting*, 2018.

[5] Gudmundsson S. The title of the conference paper. *General Aviation Aircraft Design*. Elsevier, 2014.

[6] Patterson M. D., Derlaga, J. M., Borer, N. K. High-lift propeller system configuration selection for NASA's SCEPTOR distributed electric propulsion flight demonstrator. *16th AIAA Aviation Technology, Integration, and Operations Conference*, 2016.

[7] Cole J. A., Maughmer M. D., Kinzel M. and Bramesfeld G. Higher-order free-wake method for propeller–wing systems. *Journal of Aircraft*, Vol. 56, No. 1, pp 150–165, 2019.

[8] Wang K., Zhou Z., Zhu X., and Xu X. Aerodynamic design of multi-propeller/wing integration at low Reynolds numbers. *Aerospace Science and Technology*, Vol. 84, No. 1, pp 1-17, 2019.

[9] Kroo I. Propeller-wing integration for minimum induced loss. *Journal of Aircraft*, Vol. 23, No. 7, pp 561–565, 1986.

[10] Alvarez E. J. and Ning A. Development of a vortex particle code for the modeling of wake interaction in distributed propulsion. *2018 Applied Aerodynamics Conference*, 2018.

[11] Alvarez E. J. and Ning A. Modeling multirotor aerodynamic interactions through the vortex particle method. *AIAA Aviation 2019 Forum*, 2019.

[12] Alvarez E. J. and Ning A. High-fidelity modeling of multirotor aerodynamic interactions for aircraft design. *AIAA Journal*, Vol. 58, No. 10, pp 4385-4400, 2020.

[13] Long M. *Architectural Acoustics*. 2nd edition, Elsevier, 2014.

[14] Bravo-Mosquera P. D., Cerón-Muñoz H. D., Díaz-Vázquez G. and Catalano F. M. Conceptual design and CFD analysis of a new prototype of agricultural aircraft. *Aerospace Science and Technology*, Vol. 80, pp 156-176, 2018

[15] Silva G. P. G., Eguea J. P. and Catalano F. M. Design of a Torque and Thrust Biaxial Sensor for Propellers. *26th International Congress of Mechanical Engineering (COBEM 2021)*, 2021.

[16] Štorch V., Nožička J., Brada M., Gemperle J. and Suchý J. Measurement of noise and its correlation to performance and geometry of small aircraft propellers. *EPJ Web of Conferences*, 2016.